[18] Rice, J. R., "Mathematical Aspects of Fracture," *Fracture*, Academic Press, New York, Vol. 2, 1968.
[19] McClintock, F. A., "Plasticity Aspects of Fracture," *Fracture*, Academic Press, New York, Vol. 3, 1968.
[20] McMeeking, R. M., "Large Plastic Deformation and Initiation of Fracture at the Tip of a Crack in Plane Strain," Brown University report, Providence, R. I., Dec. 1976.
[21] Shih, C. F. in *Mechanics of Crack Growth, ASTM STP 590*, American Society for Testing and Materials, 1976, pp. 3-26.
[22] Shih, C. F. and Hutchinson, J. W., "Fully Plastic Solutions and Large-Scale Yielding Estimates for Plane Stress Crack Problems," Harvard University, Rep-deap.-S-14, Cambridge, Mass., July 1975.
[23] Goldman, N. L. and Hutchinson, J. W., *International Journal of Solids and Structures*, Vol. 11, 1975, pp. 575-591.

J. W. Hutchinson[1] *and P. C. Paris*[2]

Stability Analysis of *J*-Controlled Crack Growth

REFERENCE: Hutchinson, J. W. and Paris, P. C., **"Stability Analysis of *J*-Controlled Crack Growth,"** *Elastic-Plastic Fracture, ASTM STP 668*, J. D. Landes, J. A. Begley, and G. A. Clarke, Eds., American Society for Testing and Materials, 1979, pp. 37-64.

ABSTRACT: The theoretical basis for use of the J-integral in crack growth analysis is discussed and conditions for *J*-controlled growth are obtained. Calculations related to the stability of crack growth are carried out for several deeply cracked specimen configurations. Relatively simple formulas are obtained which, in certain cases, permit an assessment of stability using data from a single load-displacement record. Numerical results for a bend specimen and for a center-cracked specimen illustrate the influence of strain-hardening and system compliance on stability.

KEY WORDS: crack propagation, fracture (materials), plastic deformation, stable crack growth

This paper builds upon the report of Paris et al [*1*][3] which promulgates an approach to the stability analysis of crack growth based on the concept of a J-integral resistance curve. We start by presenting a theoretical justification for use of the J-integral of the deformation theory of plasticity in the analysis of crack growth. Restrictions on such use are discussed in detail with particular emphasis on application in the large-scale yielding range.

When applicable, the approach of Ref *1* and the present paper is the natural extension of Irwin's resistance curve analysis (for example, see Ref *2*) for small-scale yielding based on the elastic stress intensity factor K. In a sense this approach is less fundamental, and less ambitious, than studies based on flow (that is, incremental) theories of plasticity which attempt to identify and calculate a single near-tip parameter governing the initiation and continuation of crack growth. Studies along such lines [*3,4*] have attempted to discuss the source of stable crack growth but they have not cleared the way for much progress in its analysis. In part, this is because there is not yet agreement on a suitable near-tip growth criterion; but it is

[1] Professor of applied mechanics, Harvard University, Cambridge, Mass. 02138.
[2] Professor of mechanics, Washington University, St. Louis, Mo. 63130.
[3] The italic numbers in brackets refer to the list of references appended to this paper.

also due to the difficulties of carrying out crack growth calculations using a flow theory of plasticity. Deformation theory has distinct computational advantages leading in some instances to closed-form solutions which would otherwise be unobtainable. Illustrations of this point will be found within the present paper. Moreover, the conditions for J-controlled growth are derived to ensure essentially identical results from deformation theory and flow theory on the topics herein.

Following the discussion of the applicability of J to analyzing crack growth, we discuss the stability of crack growth with emphasis on the role of the compliance of the entire system under given prescribed loading conditions. An analysis of a deeply cracked bend specimen is carried out. Relatively simple formulas are obtained for assessing stability. Numerical results for a bending specimen in plane-stress conditions are presented to illustrate the influence of strain hardening and compliance on stability. A possible scheme for measuring the resistance curve experimentally is mentioned. The final sections of the paper deal with the analyses of deeply cracked edge and center-notched specimens.

Applicability of J-Integral to Analysis of Crack Growth

Crack growth invariably involves some elastic unloading and distinctly nonproportional plastic deformation near the crack tip. The J-integral [5] is based on the deformation theory of plasticity which inadequately models both of these aspects of plastic behavior. At just a glance it would appear that use of J must be restricted to the analysis of stationary cracks. In the following, a rationale is given for use of J to analyze crack growth and stability under conditions which will be called *J-controlled growth*. The argument relies on the fact that many metals sustain only very small amounts of crack growth relative to other dimensions for overall deformations well beyond initiation of growth. If J-controlled growth is to exist, it is essential (and by implication sufficient) that nearly proportional plastic deformation occurs everywhere but in a small neighborhood of the crack tip. This results from the fact that when nearly proportional deformation occurs, the differences between a deformation theory of plasticity and the corresponding flow (incremental) theory become essentially negligible [6], and both theories are surely physically realistic.

In small-scale yielding it is widely accepted that either the elastic stress intensity factor K or J ($J = K^2$/modulus) can be used in a resistance curve analysis of stable crack growth, at least for amounts of growth which are small compared to all other relevant geometric lengths. Under limiting conditions of plane stress or plane strain the increase in crack length Δa has a unique functional relationship to K or J which is otherwise configuration-independent. In small-scale yielding the existence of such a relationship rests on the fact that K or J do uniquely measure the intensity of the fields surrounding the immediate vicinity of the crack tip. In this paper we shall be concerned mainly with growth under large-scale yielding, including fully plastic situations, where extra conditions must be met for J to be meaningful and for the relation of Δa to J to be configuration-independent. When these conditions are met, a J-resistance curve analysis is the appropriate generalization of small-scale yielding resistance curve analysis.

Figure 1 displays a schematic sketch of J versus Δa for a typical intermediate-strength steel under nominally plane-strain conditions as obtained by large-scale yielding testing techniques [7]. Leaving aside for the moment the issue of the validity of experimentally measured J-values used to generate such data, the main feature of importance to our argument in the following is the relatively large increase in J above the initiation value J_{Ic} (that is, an increase which can be as much as several times J_{Ic}) needed to produce an increase in crack length of, say, only several millimetres. Emphasis in this discussion is on this range of small growth with its attendant large increases in J. We look for conditions under which it can be expected that the dominant singularity crack-tip fields of deformation theory, with amplitude J, continue to be relevant in the presence of small amounts of growth as depicted in Fig. 2.

Consider a material with a strain hardening index n such that the plastic strain is proportional to the stress to the nth power well into the plastic range. The strain field of the dominant singularity at the crack tip according to deformation theory is [8, 9]

$$\epsilon_{ij} = k_n J^{n/(n+1)} r^{-n/(n+1)} \tilde{\epsilon}_{ij}(\theta) \tag{1}$$

where r, θ = planar-polar coordinates centered at the tip. The θ variation, $\tilde{\epsilon}_{ij}$, depends on n and on whether plane strain or plane stress pertains; k_n is a dimensional constant not needed in the present discussion. Let R denote the characteristic radius of the region controlled by Eq 1 in the deformation theory solution. In small-scale yielding, R will be some fraction of the plastic

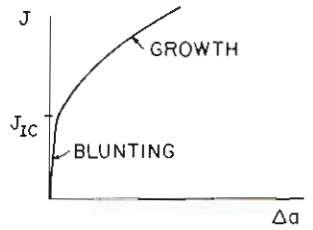

FIG. 1—*Material J-resistance curve for small amounts of crack growth.*

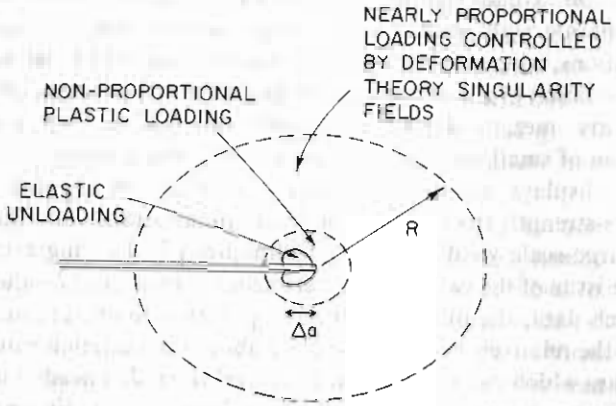

FIG. 2—*Schematic of crack tip conditions for J-controlled crack growth.*

zone size,[4] while in a fully yielded specimen R will be some fraction of the uncracked ligament. Since the wake of elastic unloading and the region of distinctly nonproportional plastic loading will be of the order Δa in length, one condition for J-controlled growth is

$$\Delta a \ll R \tag{2}$$

Next we examine the strain increments determined from deformation theory under a *simultaneous* increase in J and crack length. The crack lies along the x-axis and is assumed to advance by an amount da in the x-direction. For deformation theory, the strain field, Eq 1, continues to hold in the presence of growth with r and θ centered at the current tip location. From Eq 1, the strain increments are

$$d\epsilon_{ij} = \frac{n}{n+1} k_n J^{-1/(n+1)}\, dJ r^{-n/(n+1)} \tilde{\epsilon}_{ij}(\theta) - k_n J^{n/(n+1)}\, da\, \frac{\partial}{\partial x}\left[r^{-n/(n+1)} \tilde{\epsilon}_{ij}(\theta)\right] \tag{3}$$

Using

$$\frac{\partial}{\partial x} = \cos\theta \frac{\partial}{\partial r} - \frac{\sin\theta}{r} \frac{\partial}{\partial \theta}$$

[4] Adjusting Eq 1 to represent alternatively the elastic field, R would be substantially larger than the plastic zone size for small-scale yielding.

Eq 3 becomes

$$d\epsilon_{ij} = k_n J^{n/(n+1)} r^{-n/(n+1)} \left\{ \frac{n}{n+1} \frac{dJ}{J} \tilde{\epsilon}_{ij} + \frac{da}{r} \tilde{\beta}_{ij} \right\} \tag{4}$$

where

$$\tilde{\beta}_{ij}(\theta) = \frac{n}{n+1} \cos\theta\, \tilde{\epsilon}_{ij} + \sin\theta \frac{\partial}{\partial\theta} \tilde{\epsilon}_{ij}$$

The first term in the braces in Eq 4 corresponds to a proportional loading increment (that is, $d\epsilon_{ij} \sim \epsilon_{ij}$), while the second term is not proportional. Since $\tilde{\epsilon}_{ij}$ and $\tilde{\beta}_{ij}$ are of comparable magnitude, the first term in the braces will overwhelm the second term if

$$\frac{da}{r} \ll \frac{dJ}{J} \tag{5}$$

That is, predominantly proportional loading will occur in the dominant singularity region where Eq 5 holds.

Define a material-based length quantity D as

$$\frac{1}{D} = \frac{dJ}{da} \frac{1}{J} \tag{6}$$

where for records such as those in Fig. 1, just beyond initiation, D can be interpreted approximately as the crack advance associated with a doubling of J above J_{Ic}. Equation 5 can be restated as

$$D \ll r \tag{7}$$

If

$$D \ll R \tag{8}$$

then there exists an annular region

$$D \ll r < R \tag{9}$$

in which plastic loading is predominantly proportional *and* the singularity field, Eqs 1 or 4, is dominant. In other words, if Eq 8 is satisfied, it can be expected that there will be little difference between the strain fields predicted by flow theory and deformation theory for $r \gg D$ and, most importantly, J uniquely measures, or physically controls, the fields in the Eq 9 region surrounding the tip.

To summarize, we note that the foregoing argument is somewhat analogous to that made for the relevance of the elastic analysis for K in the presence of small-scale yielding. Here, however, the argument has dealt with two factors: (1) small-scale growth requiring Eq 2 and (2) applicability of deformation theory and J requiring Eq 8. The foregoing argument relies on the existence of some strain hardening since the θ-variation, $\tilde{\epsilon}_{ij}$, of the strain field of the dominant singularity is not unique for an ideally plastic material but will, in general, depend on the overall geometry. In effect, R diminishes to zero with vanishing strain hardening. This same point is at issue in the use of J in analyzing initiation [*10*] and has been addressed experimentally by Landes and Begley [*11*] using inherently different specimen types. In making the foregoing argument, we have also tacitly assumed that, if predominantly proportional loading occurs throughout most of the dominant singularity region, it will occur outside (that is, $r > R$) this region as well. This can be expected for the same reasons which apply to the configuration with a stationary crack under monotonic loading.

For a specimen or configuration which has fully yielded, R will be some fraction of the relevant uncracked ligament, b (or other characteristic distance from the crack tip to a boundary or loading point if smaller than b). Introduce a nondimensional parameter as defined by

$$\omega = \frac{b}{J}\frac{dJ}{da} \tag{10}$$

Thus, for a fully yielded specimen, the condition for J-controlled growth, Eq 8, can be restated

$$\omega \gg 1 \tag{11}$$

together with Eq 2.

This Eq 11 requirement for proportionality of strain in the singularity field is different than an earlier J-integral test specimen size requirement ([*7*] and discussion to Ref *11*). The earlier requirement may be stated as

$$\frac{b\sigma_0}{J} \gg 1 \tag{12}$$

where σ_0 is flow stress. This requirement, Eq 12, may be interpreted as keeping the crack opening displacement small compared to the ligament dimension, b, and is regarded as applying both to the initiation and growth phases of cracking. Indeed, perhaps both requirements must be met to maintain a proper singularity field during crack growth; however, the later one, Eq 12, will not be discussed further here.

One consequence of J-controlled growth, which follows immediately from the foregoing arguments, is that J will be approximately independent of the integration path when calculated using the standard line integral definition in conjunction with a flow (incremental) theory of plasticity as long as the points on the path satisfy (7). Shih et al [*12*] have found less than 5 percent variation in J over a wide range of paths for as much as a 5 percent increase in crack length in their finite-element analysis of a fully yielded, plane-strain compact tension specimen of A533-B steel. Using their values for b, J_{Ic}, and the initial slope dJ/da following initiation, we find that $\omega \simeq 40$ for their specimen. Shih et al [*12*] also found that their computed values of J were in good agreement with J-values obtained using the experimentally measured load-deflection curve and a deformation theory formula for a deeply cracked specimen. These two facts strongly suggest that J-controlled growth is in evidence in their specimens. An important question which remains to be answered is, What is the *smallest* value of ω which will guarantee J-controlled growth? To a certain extent the answer will depend on specimen configuration and on strain hardening. Closely related is the need for a systematic study of the amount of growth allowable under J-controlled conditions.

An additional consequence of J-controlled growth is that the material resistance curve of J versus Δa obtained under large-scale yielding conditions must coincide with that obtained under small-scale yielding conditions, assuming that the same plane-strain or plane-stress conditions prevail in both instances. [As discussed earlier, a relation of J (or K) versus Δa in small-scale yielding can be meaningful independent of the condition of Eq 8.]

Stability of J-Controlled Growth

Elaborating further in the development of Paris et al [*1*], we derive some general expressions related to growth and stability based on a J-resistance curve analysis.

Consider a two-dimensional specimen (in plane strain or plane stress) with a straight crack of length a and of a material characterized by deformation theory. As depicted in Fig. 3, let P be the generalized load acting on the specimen and let Δ be the load point displacement of the specimen through which P works. The specimen is loaded in series with a linear spring with compliance C_M (which can, if desired, be identified with the testing machine compliance) such that the total load point displacement is

$$\Delta_T = C_M P + \Delta \tag{13}$$

Let J have the usual deformation theory definition [*5*], equivalently as the path-independent line integral, or as

$$J = \int_0^P \left(\frac{\partial \Delta}{\partial a}\right)_P dP = -\int_0^\Delta \left(\frac{\partial P}{\partial a}\right)_\Delta d\Delta \tag{14}$$

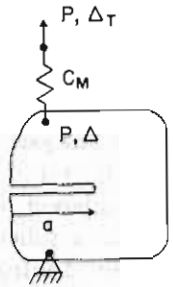

FIG. 3—*Typical specimen geometry.*

It will be important to draw a distinction between applied values of J and the values of J on the material resistance curve such as that in Fig. 1. For this purpose, values of J falling on the material resistance curve will be denoted by J_{mat} and will be regarded as a function solely of the increase in crack length Δa. For given material properties and overall specimen geometry, the "applied" J in Eq 14 can be regarded as a function of P and current crack length $a = a_0 + \Delta a$, where a_0 is the initial crack length. At any P and current length, a, equilibrium based on the resistance curve data requires

$$J(a, P) = J_{mat}(\Delta a) \tag{15}$$

Stability will be considered with the total load point displacement Δ_T held fixed. (Then, note that $C_M = 0$ corresponds to a rigid test machine while $C_M = \infty$ corresponds to a dead-load machine.) Stability of the equilibrium state, Eq 15, will be ensured if

$$\left(\frac{\partial J}{\partial a}\right)_{\Delta_T} < \frac{dJ_{mat}}{da} \tag{16}$$

The Eq 15 state is assumed to be unstable if

$$\left(\frac{\partial J}{\partial a}\right)_{\Delta_T} > \frac{dJ_{mat}}{da} \tag{17}$$

and the onset of instability is associated with equality in Eq 16 or 17. Following Ref *1* we introduce nondimensional quantities

$$T = \frac{E}{\sigma_0^2}\left(\frac{\partial J}{\partial a}\right)_{\Delta_T} \quad \text{and} \quad T_{mat} = \frac{E}{\sigma_0^2}\frac{dJ_{mat}}{da} \tag{18}$$

where E is Young's modulus and σ_0 is an appropriate flow stress. In terms of these quantities, Eqs 16 and 17 become

$$T < T_{mat} \text{ (stability)} \tag{19}$$

$$T > T_{mat} \text{ (instability)} \tag{20}$$

A general expression for $(\partial J/\partial a)_{\Delta_T}$, to be used in later sections, will now be derived by regarding J and Δ as functions of a and P. For arbitrary da and dP

$$dJ = \left(\frac{\partial J}{\partial a}\right)_P da + \left(\frac{\partial J}{\partial P}\right)_a dP \tag{21}$$

But with Δ_T held fixed, from Eq 13

$$d\Delta_T = C_M\, dP + \left(\frac{\partial \Delta}{\partial a}\right)_P da + \left(\frac{\partial \Delta}{\partial P}\right)_a dP = 0$$

and thus

$$dP = -\, da \left(\frac{\partial \Delta}{\partial P}\right)_P \left[C_M + \left(\frac{\partial \Delta}{\partial P}\right)_a\right]^{-1} \tag{22}$$

Combining Eqs 21 and 22 gives

$$\left(\frac{\partial J}{\partial a}\right)_{\Delta_T} = \left(\frac{\partial J}{\partial a}\right)_P - \left(\frac{\partial J}{\partial P}\right)_a \left(\frac{\partial \Delta}{\partial a}\right)_P \left[C_M + \left(\frac{\partial \Delta}{\partial P}\right)_a\right]^{-1} \tag{23}$$

If C_M is identified with the compliance of the testing machine, then specialization to the two limiting cases noted in the foregoing can be made. With $C_M = 0$, Eq 23 applies to a rigid test machine. If $C_M \to \infty$, the test machine applies a dead load and Eq 23 reduces to

$$\left(\frac{\partial J}{\partial a}\right)_{\Delta_T} = \left(\frac{\partial J}{\partial a}\right)_P \tag{24}$$

Analysis of Deeply Cracked Bend Specimen

In the spirit of Rice, Paris, and Merkle [*13*], a formula will be derived for $(\partial J/\partial a)_{\Delta_T}$ for a deeply cracked bend specimen which, up to initiation, involves quantities that can be taken from a single experimental test record. First, however, we derive a more general result for J than that given in Ref *13*, which allows for determination of J under changing crack length. In the configuration of Fig. 4*a*, M is the applied moment per unit thickness, a is the current crack length, and a_0 is the initial crack length. The specimen

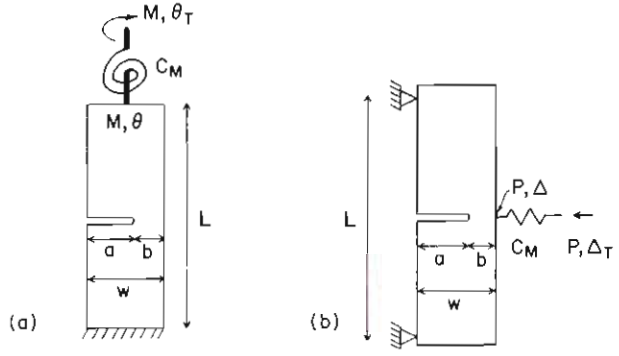

FIG. 4—*Bend specimen* (a) *and three-point bend specimen* (b).

load-point rotation θ at any given M can be decomposed into two parts according to

$$\theta = \theta_{nc} + \theta_c \tag{25}$$

where θ_{nc}, by definition, is the rotation of the uncracked specimen under the same M, and θ_c is the remainder (that is, the contribution due to the presence of the crack). It is assumed that the current ligament length $b = W - a$ is sufficiently small compared with W such that θ_c at a given M depends only on b and not on L or W. From dimensional considerations it then follows that θ_c must be a function of the combination M/b^2, that is

$$\theta_c = f(M/b^2) \text{ or } M = b^2F(\theta_c) \tag{26}$$

In Ref *13* it is noted that Eq 26 implies

$$\left(\frac{\partial\theta}{\partial a}\right)_M = \left(\frac{\partial\theta_c}{\partial a}\right)_M = \frac{2M}{b}\left(\frac{\partial\theta_c}{\partial M}\right)_a \tag{27}$$

Using Eq 27 in the definition of J from the first form of Eq 14, that is

$$J = \int_0^M \left(\frac{\partial\theta}{\partial a}\right)_M dM \tag{28}$$

gives

$$J = \frac{2}{b}\int_0^{\theta_c} M d\theta_c = 2b\int_0^{\theta_c} F(\theta_c)\, d\theta_c \tag{29}$$

However, it is noted here that using the second form of Eq 14 with the second

form of Eq 26 leads to this same result (Eq 29) more directly. The definition of J in Eq 28 and the derivation leading to Eq 29 require a to be held fixed in the integration. Nevertheless, by virtue of its deformation theory definition, $J(a, \theta_c)$ is independent of the history, giving rise to the current values of a and θ_c. (Equivalently, J can be regarded as a function of a and M, but for present purposes θ_c is a more convenient independent variable.) For arbitrary increments in a and θ_c it follows from Eq 29 that

$$\begin{aligned} dJ &= 2bd\theta_c F(\theta_c) - 2da\int_0^{\theta_c} F(\theta)\, d\theta_c \\ &= \frac{2M}{b}\, d\theta_c - \frac{J}{b}\, da \end{aligned} \tag{30}$$

Since dJ is a perfect differential, the general expression for J from Eq 30, that is

$$J = 2\int_0^{\theta_c} \frac{M}{b}\, d\theta_c - \int_{a_0}^{a} \frac{J}{b}\, da \tag{31}$$

holds for any history of a and θ_c leading to the current values and is necessarily independent of the history. With no change in crack length, Eq 31 reduces to Eq 29. In the presence of growth, the second term represents a correction to Eq 29 which should be but is not currently used to determine J from experimental data [*7,11*]. For small amounts of growth, this correction is usually small but not necessarily negligible. In addition, b should take on its variable value in the first term in Eq 31.

As in the general discussion in the previous section, let C_M be the compliance of a linear spring in series with the bend specimen. The total load point rotation is given by

$$\theta_T = C_M M + \theta = C_M M + \theta_{nc} + \theta_c \tag{32}$$

To obtain an expression for $(\partial J/\partial a)_{\theta_T}$, it is first necessary to evaluate $(\partial J/\partial a)_M$. From Eq 28

$$\left(\frac{\partial J}{\partial a}\right)_M = \int_0^M \left(\frac{\partial^2\theta}{\partial a^2}\right)_M dM \tag{33}$$

Using Eq 26, it is readily verified that

$$\left(\frac{\partial^2\theta}{\partial a^2}\right)_M = \left(\frac{\partial^2\theta_c}{\partial a^2}\right)_M = \frac{6M}{b^2}\left(\frac{\partial\theta_c}{\partial M}\right)_a + \frac{4M^2}{b^2}\left(\frac{\partial^2\theta_c}{\partial M^2}\right)_a \tag{34}$$

from which it follows that

$$\left(\frac{\partial J}{\partial a}\right)_M = 6 \int_0^{\theta_c} \frac{M}{b^2}\, d\theta_c + 4 \int_0^{\theta_c} \frac{M^2}{b^2} \left(\frac{\partial^2 \theta_c}{\partial M^2}\right)_a dM \tag{35}$$

Here again it is important to note that $(\partial J/\partial a)_M$ depends only on the current values of a and θ_c or M. In Eq 35 it is understood that the integrals are to be evaluated with a held fixed at the current value. The first term in Eq 35 is $3J/b$. The second term can be integrated by parts and combined with the first to give

$$\left(\frac{\partial J}{\partial a}\right)_M = -\frac{J}{b} + \frac{4M^2}{b^2} \left(\frac{\partial \theta_c}{\partial M}\right)_a \tag{36}$$

For the bend specimen, the general expression, Eq 23, translates to

$$\left(\frac{\partial J}{\partial a}\right)_{\theta_T} = \left(\frac{\partial J}{\partial a}\right)_M - \left(\frac{\partial J}{\partial M}\right)_a \left(\frac{\partial \theta_c}{\partial a}\right)_M \left[C_M + \left(\frac{\partial \theta}{\partial M}\right)_a\right]^{-1} \tag{37}$$

This expression can be substantially simplified without approximation using Eqs 27 and 36

$$\left(\frac{\partial J}{\partial M}\right)_a = \frac{2}{b} M \left(\frac{\partial \theta_c}{\partial M}\right)_a \tag{38}$$

and

$$\left(\frac{\partial \theta}{\partial M}\right)_a = \frac{d\theta_{nc}}{dM} + \left(\frac{\partial \theta_c}{\partial M}\right)_a \equiv C_{nc} + \left(\frac{\partial \theta_c}{\partial M}\right)_a \tag{39}$$

Here C_{nc} is the compliance of the uncracked specimen. In general, C_{nc} may be a function of M, but for a deeply cracked specimen it will usually be the elastic compliance since M will seldom exceed initial yield of the uncracked specimen. The resulting exact reduction of Eq 37 is

$$\left(\frac{\partial J}{\partial a}\right)_{\theta_T} = -\frac{J}{b} + \frac{4M^2}{b^2} \left[\frac{C}{1 + C\left(\frac{\partial M}{\partial \theta_c}\right)_a}\right] \tag{40}$$

where C is the combined compliance

$$C = C_M + C_{nc} \tag{41}$$

In a rigid machine, $C_M = 0$ and Eq 40 applies with $C = C_{nc}$. In a dead-load machine, $C_M \to \infty$ and Eq 40 reduces to the expression for $(\partial J/\partial a)_M$ in Eq 36. For a fully yielded, elastic-perfectly plastic specimen, M is the limit

moment which is independent of θ_c for fixed a, so that Eq 40 becomes very simply just

$$\left(\frac{\partial J}{\partial a}\right)_{\theta_T} = -\frac{J}{b} + \frac{4M^2 C}{b^2} \tag{42}$$

The analysis of the three-point bend specimen of Fig. 4*b* is essentially identical to that carried out in the foregoing. Now Δ_T is the total load point displacement through which P works and Δ_C is the displacement of the specimen due to the presence of the crack defined similarly to Eq 25. With C as the combined compliance, now as

$$C = C_M + \frac{d\Delta_{nc}}{dP} \equiv C_M + C_{nc}$$

one finds

$$\left(\frac{\partial J}{\partial a}\right)_{\Delta_T} = -\frac{J}{b} + \frac{4P^2}{b^2} \left[\frac{C}{1 + C\left(\frac{\partial P}{\partial \Delta_C}\right)_a}\right] \tag{43}$$

Both Eqs 40 and 43 are exact for deeply cracked specimens. It is now possible to make contact with the simpler approximate analysis of a fully yielded, elastic-perfectly plastic three-point bend specimen given by Paris et al [*1*]. At the limit state, $M = PL/4 = A\sigma_0 b^2$, where σ_0 is the tensile yield stress and $A \simeq 0.35$ for plane strain and $A \simeq 0.27$ for plane stress. In a rigid testing machine, $C = C_{nc} = L^3/(4EW^3)$. Under these circumstances, Eq 43 immediately leads to

$$T = \frac{E}{\sigma_0^2} \left(\frac{\partial J}{\partial a}\right)_{\Delta_T} = 16A^2 \frac{b^2 L}{W^3} - \frac{EJ}{\sigma_0^2 b} \tag{44}$$

The first term in Eq 44 is the same as that obtained in Ref *1*, while the second term has been approximated in the analysis of Ref *1*.

Prior to the initiation of crack growth, Eqs 40 and 43 involve quantities which can all be obtained from a single test record. Furthermore, all quantities on the right-hand side of Eqs 40 and 43 are continuous across the initiation point and, thus, so are $(\partial J/\partial a)_{\theta_T}$ and $(\partial J/\partial a)_{\Delta_T}$. It follows that stability of crack growth initiation can be assessed using Eqs 40 or 43 from quantities obtained directly from the experimental test record just prior to initiation. For a fully yielded specimen with little strain hardening, it may be possible in some instances to neglect $C(\partial M/\partial \theta_c)_a$ in Eq 40 (or the analogous term in Eq 43 and thereby use Eq 42). When this term is not negligible, it will

be necessary to estimate $(\partial M/\partial\theta_c)_a$ in order to assess stability using Eq 40 beyond the initiation of crack growth.

Numerical Results for a Deeply Cracked Bend Specimen in Plane Stress

The estimation procedure of Shih and Hutchinson [*14*] will be used to relate J and θ_c to M for the deeply cracked, plane stress bend specimen of Fig. 4*a*. These relations are then sufficient to calculate $(\partial J/\partial a)_{\theta_T}$ using Eq 40. The material is assumed to be governed by a Ramberg-Osgood stress-strain curve in uniaxial tension, that is

$$\epsilon/\epsilon_O = \sigma/\sigma_0 + \alpha(\sigma/\sigma_0)^n \tag{45}$$

where σ_0 is the effective yield stress and $\epsilon_O = \sigma_0/E$. The estimation procedure uses the linear elastic solution and a fully plastic power-law solution, which is given in Ref *14*, to interpolate over the entire range from small-scale yielding to fully yielded conditions.

The results of the procedure as applied to the deeply cracked plane stress bend specimen are

$$\frac{EJ}{\sigma_0^2 b} = 1.135\psi^3\left(\frac{M}{M_O}\right)^2 + \alpha h_1(n)\left(\frac{M}{M_O}\right)^{n+1} \tag{46}$$

$$\frac{\theta_c}{\epsilon_0} = 4.238\psi^2\left(\frac{M}{M_O}\right) + \alpha h_3(n)\left(\frac{M}{M_O}\right)^n \tag{47}$$

where $M_O = A\sigma_0 b^2$ and $A = 0.27$. The plasticity adjustment for the effective crack length in the low M range is incorporated through the ψ factor [*14*], which for the deeply-cracked specimen is given by

$$\frac{1}{\psi} = \frac{b_{\text{eff}}}{b} = 1 - 0.1806\left(\frac{n-1}{n+1}\right)\left(\frac{M}{M_O}\right)^2, \qquad M \le M_O \tag{48}$$

$$= 1 - 0.1806\left(\frac{n-1}{n+1}\right), \qquad M \ge M_O \tag{49}$$

The numerical coefficients in the first terms in Eqs 46 and 47 and in Eq 48 are from the appropriate deeply cracked limits for the linear elastic problems which can be found in Ref *15*. For $h_1(n)$ and $h_3(n)$ we have used the numerical values presented in Table 2 of Ref *14* which were computed for $b/W = 1/2$. (These are listed again in Table 1 of the present paper.) As discussed in Ref *14*, these values are expected to be very close to the deeply-cracked limit for $b/W \to 0$ when $n \ge 3$.

TABLE 1—*Numerical values for* $h_1(n)$ *and* $h_3(n)$, *taken from Ref* 14.

	$n = 2$	$n = 3$	$n = 5$	$n = 10$
Bend				
$h_1(n)$	0.957	0.851	0.717	0.551
$h_3(n)$	2.36	2.03	1.59	1.12
Center-cracked				
$h_1(n)$	...	1.09	0.906	0.717
$h_3(n)$	...	1.93	1.35	0.88

From Eqs 47 and 48

$$\frac{M_O}{\epsilon_0}\left(\frac{\partial\theta_c}{\partial M}\right)_a = 4.238\psi^2 + 3.062\psi^3\left(\frac{n-1}{n+1}\right)\left(\frac{M}{M_O}\right)^2 + \alpha n h_3(n)\left(\frac{M}{M_O}\right)^{n-1} \tag{50}$$

for $M \le M_O$. For $M > M_O$ we take

$$\frac{M_O}{\epsilon_0}\left(\frac{\partial\theta_c}{\partial M}\right)_a = 4.238\psi^2 + 3.062\psi^3\left(\frac{n-1}{n+1}\right) + \alpha n h_3(n)\left(\frac{M}{M_O}\right)^{n-1} \tag{51}$$

The second term in Eq 51 would be absent if we had used Eq 49. It is included to ensure continuity of $(\partial\theta_c/\partial M)_a$ at $M = M_O$. Both this quantity and $(\partial J/\partial M)_a$ are discontinuous across $M = M_O$ according to the estimation procedures of Ref *14*, leading to Eqs 46–49, where in fact these two quantities should be continuous. In this paper, where we are primarily interested in displaying the trends due to strain hardening, the effect of including or omitting the second term in Eq 51 makes relatively little difference. For future work, however, the estimation procedure will need to be improved upon in this regard.

Equation 40 can be written in nondimensional form as

$$T = \frac{E}{\sigma_0^2}\left(\frac{\partial J}{\partial a}\right)_{\theta_T} = -\frac{EJ}{\sigma_0^2 b} + 4A^2\left(\frac{M}{M_O}\right)^2\bar{C}\left[1 + A\bar{C}\frac{\epsilon_0}{M_O}\left(\frac{\partial M}{\partial\theta_c}\right)_a\right]^{-1} \tag{52}$$

where $\bar{C} = Eb^2C = Eb^2(C_M + C_{nc})$ is the nondimensional combined com-

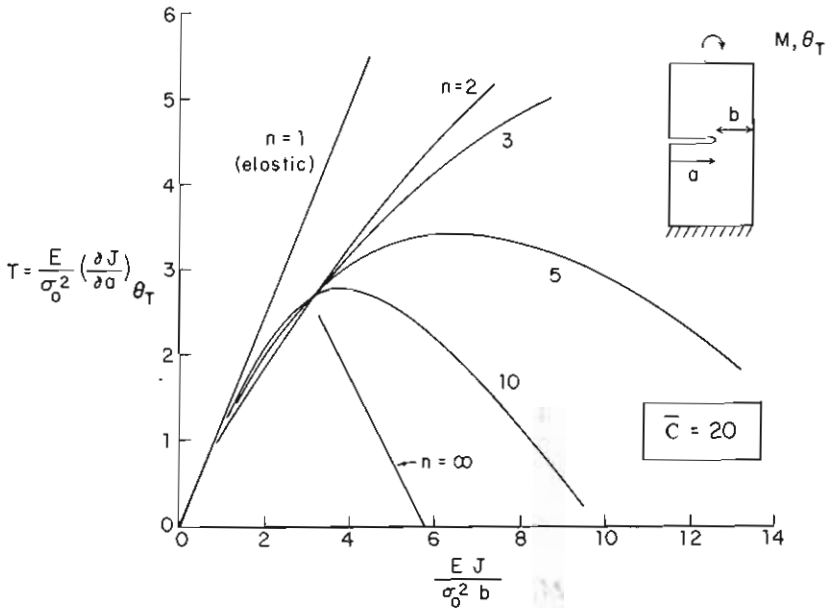

FIG. 5—*Numerical results for* T *versus* EJ/(σ_0^2b) *for a deeply cracked plane-stress bend specimen for various values of the strain hardening index* n. *Nondimensional combined compliance is* $\bar{C} = 20$, *corresponding to a typically dimensioned specimen in a rigid test machine (see text).*

pliance. Values of T and $EJ/(\sigma_0^2 b)$ for values of M/M_O are generated using Eqs 46-52. We have taken $\alpha = 3/7$ for $n > 1$ and for $n = 1$ we have used the linear elastic formulas. In Figs. 5 and 6 we have cross-plotted T as a function of $EJ/(\sigma_0^2 b)$ for various values of the hardening index n. The curve in Fig. 5 labeled $n = \infty$ is obtained from the fully yielded result, Eq 42, for the elastic-perfectly plastic specimen, that is

$$T = -\frac{EJ}{\sigma_0^2 b} + 4A^2\bar{C} \tag{53}$$

Fully yielded conditions set in when $M > M_O$ and this occurs when $EJ/(\sigma_0^2 b)$ is a bit larger than 2 for essentially all the higher n-values.

For the bend specimen of Fig. 4*a*

$$Eb^2C_{nc} = 12Lb^2/W^3 \tag{54}$$

The results in Fig. 5 are for a combined nondimensional compliance $\bar{C} = 20$. In a rigid test machine, this corresponds to a specimen with $Lb^2/W^3 = 5/3$, which is representative of a typical test specimen. For $n \geq 5$, it can be seen

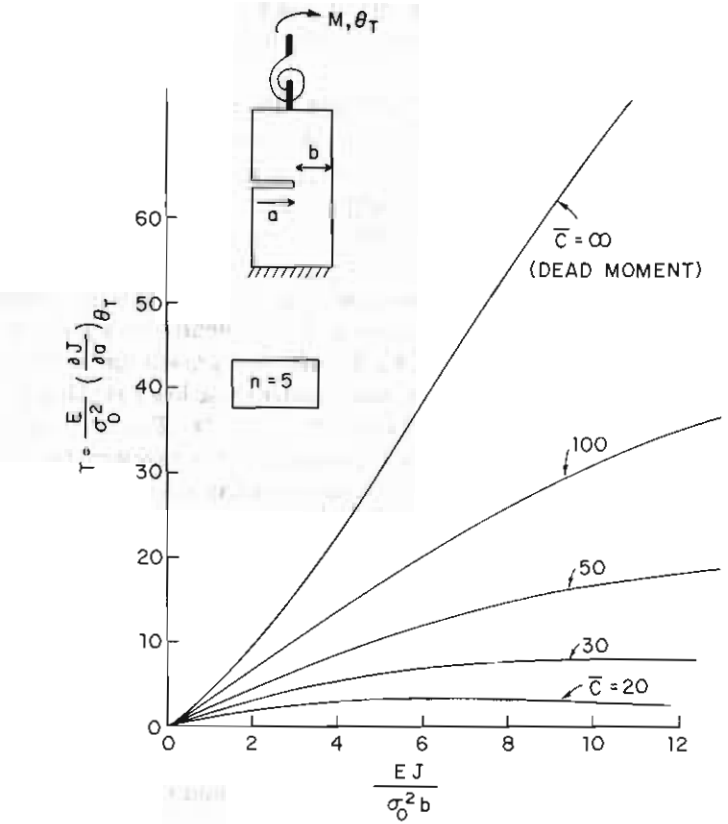

FIG. 6—*Influence of combined compliance* $\bar{C}$ *on* T *for plane-stress bend specimen for strain hardening index* n = 5.

from Fig. 5 that T will always be less than about 4 in plane stress. Fully plastic power-law solutions for bend specimens are not yet available for plane strain. However, judging from Eqs 52 and 53, we can perhaps expect T-values to be larger in plane strain by a factor of as much as 2, due to the presence of A^2. Thus it is reasonable to expect that T will always be less than some number around 10 in plane strain when $\bar{C} = 20$ and when $n \geq 5$. In contrast, T_{mat} spans the range $1 < T_{mat} < 200$ for a wide range of steels under nominally plane-strain conditions just following initiation (Ref *1*, Appendix II). Thus, only those specimens of steels in the low end of the range of T_{mat} will display unstable crack growth upon crack growth initiation in a bend specimen rigid test machine (compare Eqs 18 and 19).

The effect of increasing the combined compliance $\bar{C}$ is seen in Fig. 6 for $n = 5$. The lowest curve is from Fig. 5. The uppermost curve is for $\bar{C} = \infty$, corresponding to a specimen loaded under dead (constant) moment. Paris et al ([*1*], Part II) varied the combined compliance in their test program by in-

cluding an extra bar in series with a three-point bend specimen. In this way they were able to achieve a tenfold increase in compliance with the associated large increase in T.

The parameter ω in Eq 10 related to the validity of J-controlled growth in the fully yielded range can be expressed in the revealing form

$$\omega = \left(\frac{\sigma_0^2 b}{EJ}\right) T \tag{55}$$

involving only the ordinate and abscissa of Figs. 5 and 6. For the results of Fig. 5 for $\overline{C} = 20$, ω does not exceed unity. Consequently, as a result of Eq 11, it is unlikely that the conditions for J-controlled growth are satisfied for an increment of crack growth with θ_T fixed under these low compliance conditions. This should be no cause for concern if $T_{mat} \gg T$ since then crack growth is almost certainly highly stable anyway. The parameter T in Eq 55 increases with increasing compliance. At the compliance associated with the onset of instability

$$\omega = \left(\frac{\sigma_0^2 b}{EJ}\right) T_{mat} \tag{56}$$

In the plane-strain tests of Paris et al ([*1*], Part II), $T_{mat} \simeq 36$ and $\omega \simeq 15$, using Eq 56 with $J = J_{Ic}$.

Two-Specimen Method for Determining (dJ_{mat}/da) and $(\partial M/\partial\theta_c)_a$ in J-Controlled Growth

Here we note a method which, in principle, can be used to measure (dJ_{mat}/da) without recourse to direct measurement of crack length changes. It will permit an experimental determination of $(\partial M/\partial\theta_c)_a$ once growth starts.

Consider two deeply cracked bend specimens of identical material, denoted by A and B, with differing initial ligament lengths $b_A{}^o$ and $b_B{}^o$. Equation 26 applies to both specimens, that is

$$M_A = b_A{}^2 F(\theta_c) \text{ and } M_B = b_B{}^2 F(\theta_c) \tag{57}$$

where b_A and b_B are the current ligaments. The $F(\theta_c)$ in each of Eqs 57 are the same since $F(\theta_c)$ depends only on material properties. Thus at the same value of θ_c, from Eq 29

$$J_A/J_B = b_A/b_B \tag{58}$$

Consequently, initiation, that is, $J = J_{Ic}$, will occur at a larger value of θ_c for

Specimen A than for Specimen B, if $b_A{}^o < b_B{}^o$. With $b_A{}^o < b_B{}^o$, Specimen A can be used to measure $F(\theta_c)$ from

$$F(\theta_c) = M_A/(b_A{}^o)^2 \tag{59}$$

in the range of θ_c prior to initiation in A, as depicted in Fig. 7.

In Fig. 7 we have also depicted the curve of $M_B/(b_B{}^o)^2$ versus θ_c, where $(b_B{}^o)$ is the initial ligament of B. Prior to initiation in B, the two curves in Fig. 7 must coincide, assuming both specimens have the same material and same degree of plane-strain constraint. From the second equation in Eq 57

$$dM_B = 2b_B\, db_B F + b_B{}^2 F'\, d\theta_c$$

where $F' = dF/d\theta_c$. With $da = -db_B$ the foregoing equation can be rearranged to give

$$da = \frac{b_B}{2}\left[\frac{F'(\theta_c)}{F(\theta_c)}\, d\theta_c - \frac{dM_B}{M_B}\right] \tag{60}$$

This equation provides a relation for indirectly obtaining increments in crack length in Specimen B in terms of the measured relation between M_B and θ_c and from $F(\theta_c)$ determined by using A. The associated change in J_B, that is, $dJ_B = dJ_{mat}$, is given by Eq 30. Combining Eqs 60 and 30 gives

$$\frac{dJ_{mat}}{da} = 4F(\theta_c)\left[\frac{F'(\theta_c)}{F(\theta_c)} - \frac{1}{M_B}\left(\frac{dM_B}{d\theta_c}\right)\right]^{-1} - \frac{J_B}{b_B} \tag{61}$$

These results, Eqs 60 and 61, may be used to assess crack length changes, da, and dJ_{mat}/da up to values of θ_c where initiation occurs in Specimen A, or

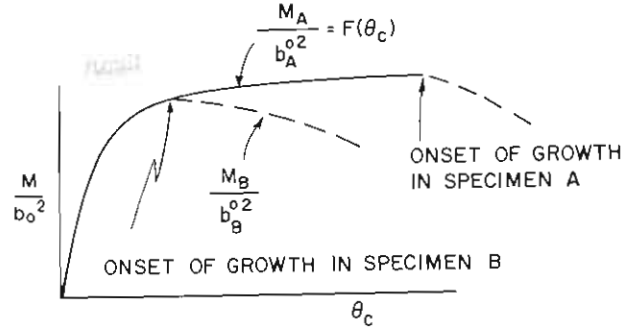

FIG. 7—*Curves of normalized moment as a function of θ_c for two deeply cracked bend specimens with differing initial uncracked ligaments* ($b_A{}^o < b_B{}^o$).

$J_A = J_{Ic}$. This limit can be assessed from the onset of growth in Specimen B, where $J_B = J_{Ic}$, and using Eqs 29 and 58.

The practicality of using Eqs 60 and 61 together with experimental records must await further work.[5] One desirable feature of these relations is that the resistance curve data, dJ_{mat}/da versus Δa, are generated without having to specify a precise definition of initiation.

Using Eq 57 we also note that

$$\left(\frac{\partial M_B}{\partial \theta_c}\right)_a = b_B{}^2 F'(\theta_c) \tag{62}$$

Thus $F'(\theta_c)$ obtained from Specimen A also provides the one term in the general expression, Eq 40, for $(\partial J/\partial a)_{\theta_T}$ which cannot be obtained from Specimen B itself. For small amounts of growth, the replacement of b_B by its initial value in Eqs 60-62 will introduce little error.

Analysis of Deeply Cracked Center-Notched and Edge-Notched Specimens Under Tension

In this section, expressions are obtained for $(\partial J/\partial a)_{\Delta_T}$ for deeply cracked center and edge-notched specimens in plane strain or plane stress and for the deeply cracked round bar. First the two-dimensional plane specimens in Fig. 8*a* and *b* will be considered. In each case we now write the load-point displacement of the specimen Δ as the sum of the elastic part Δ_e and the plastic part Δ_P according to

$$\Delta = \Delta_e + \Delta_P \tag{63}$$

For $b/w \ll 1$, dimensional analysis implies the general functional dependence

$$\Delta_P = bf(P/b) \tag{64}$$

where P is the load per unit thickness carried by each ligament. Let

$$J_e = \int_0^P \left(\frac{\partial \Delta_e}{\partial a}\right)_P dP \tag{65}$$

denote the value of J for an elastic specimen at P. Then

$$J = \int_0^P \left(\frac{\partial \Delta}{\partial a}\right)_P dP = J_e + \int_0^P \left(\frac{\partial \Delta_P}{\partial a}\right)_P dP \tag{66}$$

[5]Although these methods were used in Ref *1*, Part II, for data reduction, their full application and limitations to practical testing procedures are yet to be explored.

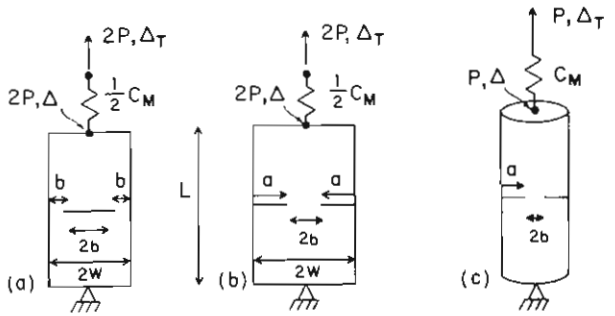

FIG. 8—*Center-cracked specimen* (a), *edge-cracked specimen* (b), *and edge-cracked round bar specimen* (c).

Using Eq 64 and following the development in Ref *13*, one can show that

$$J = J_e + b^{-1}\left\{2\int_0^{\Delta_P} P d\Delta_P - P\Delta_P\right\} \tag{67}$$

Next using Eqs 64 and 66 we find

$$\left(\frac{\partial J}{\partial a}\right)_P = \left(\frac{\partial J_e}{\partial a}\right)_P + \int_0^P \frac{P^2}{b^2}\left(\frac{\partial^2 \Delta_P}{\partial P^2}\right)_a dP \tag{68}$$

But for deeply cracked specimens

$$J_e = kP^2/(2bE) \tag{69}$$

where

$k = (1 - \nu^2)8\pi/(\pi^2 - 4)$ (plane strain, center-notched)
$= 8\pi/(\pi^2 - 4)$ (plane stress, center-notched)
$= (1 - \nu^2)8/\pi$ (plane strain, edge-notched)
$= 8/\pi$ (plane stress, edge-notched)

and where ν is Poisson's ratio.

So, $(\partial J_e/\partial a)_P = J_e/b$. Integrating the second term in Eq 68 by parts and using Eq 66 gives

$$\left(\frac{\partial J}{\partial a}\right)_P = -\frac{J}{b} + \frac{2J_e}{b} - \frac{P\Delta_P}{b^2} + \frac{P^2}{b^2}\left(\frac{\partial \Delta_P}{\partial P}\right)_a \tag{70}$$

With 1/2 C_M as the compliance of a linear spring in series with the specimen, the total load point displacement is

$$\Delta_T = C_M P + \Delta = C_M P + \Delta_e + \Delta_P \tag{71}$$

To reduce the general expression, Eq 23, for $(\partial J/\partial a)_{\Delta_T}$, we note the following relations

$$\left(\frac{\partial \Delta_P}{\partial a}\right)_P = -\frac{\Delta_P}{b} + \frac{P}{b}\left(\frac{\partial \Delta_P}{\partial P}\right)_a$$

$$\left(\frac{\partial \Delta_e}{\partial a}\right)_P = \frac{kP}{Eb} = \frac{2J_e}{P}$$

Let $C_e = (\partial \Delta_e/\partial P)_a$ be the compliance of the cracked elastic half-specimen and denote by C the combined elastic compliance

$$C = C_e + C_M \tag{72}$$

Then Eq 23 can be reduced by algebraic manipulation without approximation to

$$\left(\frac{\partial J}{\partial a}\right)_{\Delta_T} = -\frac{J}{b} + \left[\frac{2J_e}{b} - \frac{P\Delta_P}{b^2} + \frac{P^2}{b^2}\left(\frac{\partial \Delta_P}{\partial P}\right)_a\right] \times \left[C - \frac{k}{E} + \frac{\Delta_P}{P}\right] \times \left[C + \left(\frac{\partial \Delta_P}{\partial P}\right)_a\right]^{-1} \tag{73}$$

In a dead-load machine, $C = \infty$ and Eq 73 reduces to $(\partial J/\partial a)_P$. For a fully yielded, elastic-perfectly plastic specimen, P is at the limit load and $(\partial P/\partial \Delta_p)_a = 0$ so that Eq 73 becomes

$$\left(\frac{\partial J}{\partial a}\right)_{\Delta_T} = -\frac{J}{b} + \frac{P^2}{b^2}\left(C - \frac{k}{E} + \frac{\Delta_P}{P}\right) \tag{74}$$

The same comments made in connection with the analogous formulas for the bend specimen apply here; namely, Eq 73 allows determination of $(\partial J/\partial a)_{\Delta_T}$ from a single experimental record prior to initiation. Furthermore, $(\partial J/\partial a)_{\Delta_T}$ is continuous across the point of initiation. Beyond initiation, $(\partial P/\partial \Delta_P)_a$ must be estimated or perhaps neglected, as in Eq 74, if the specimen is fully yielded and strain hardening is not significant.

For the deeply cracked edge-notched round bar of Fig. 8*c* we write, copying the procedure for the bend specimen

$$\Delta_T = C_M P + \Delta = C_M P + \Delta_{nc} + \Delta_c \tag{75}$$

Now, with b as the radius of the circular ligament

$$\Delta_c = bf(P/b^2) \tag{76}$$

where P is the total load. Omitting details, we find

$$J = \frac{1}{2\pi b^2}\left[3\int_0^{\Delta_c} P d\Delta_c - P\Delta_c\right] \tag{77}$$

$$\left(\frac{\partial J}{\partial a}\right)_P = -\frac{J}{b} - \frac{P\Delta_c}{\pi b^3} + \frac{2}{\pi b^3}P^2\left(\frac{\partial \Delta_c}{\partial P}\right)_a \tag{78}$$

$$\left(\frac{\partial J}{\partial a}\right)_{\Delta_T} = -\frac{J}{b} - \frac{P\Delta_c}{\pi b^3} + \frac{1}{2\pi b^3}\left[4P^2C + 4P\Delta_c - \Delta_c^2\left(\frac{\partial P}{\partial \Delta_c}\right)_a\right] \times \left[1 + C\left(\frac{\partial P}{\partial \Delta_c}\right)_a\right]^{-1} \tag{79}$$

where

$$C = \frac{d\Delta_{nc}}{dP} + C_M \tag{80}$$

For a fully yielded, elastic-perfectly plastic specimen, Eq 79 reduces to

$$\left(\frac{\partial J}{\partial a}\right)_{\Delta_T} = -\frac{J}{b} + \frac{P\Delta_c}{\pi b^3} + \frac{2P^2C}{\pi b^3} \tag{81}$$

Numerical Results for a Deeply Cracked Center-Notched Specimen in Plane Stress

We again employ the estimation procedure of Ref *14* together with the general formula, Eq 73, to generate numerical results for T for the deeply cracked center-notched specimen of Fig. 8*a*. The Ramberg-Osgood stress-strain curve, Eq 45, is used. Of the quantities needed in Eq 73, J_e has been given previously while J and Δ_P are

$$\frac{EJ}{\sigma_0^2 b} = \frac{k}{2}\psi\left(\frac{P}{P_O}\right)^2 + \alpha h_1(n)\left(\frac{P}{P_O}\right)^{n+1} \tag{82}$$

$$\frac{\Delta_P}{\epsilon_0 b} = k\ln\psi\left(\frac{P}{P_O}\right) + \alpha h_3(n)\left(\frac{P}{P_O}\right)^n \tag{83}$$

where $P_O = \sigma_0 b$ and

$$\frac{1}{\psi} = \frac{b_{eff}}{b} = 1 - \frac{k}{4\pi}\left(\frac{n-1}{n+1}\right)\left(\frac{P}{P_O}\right)^2, \quad P \le P_O$$
$$= 1 - \frac{k}{4\pi}\left(\frac{n-1}{n+1}\right), \quad P \ge P_O \tag{84}$$

The linear elastic solution for the limit of a deeply cracked specimen from Ref *15* has been used to arrive at the first terms in Eq 82 and ψ; the first term in Eq 83 follows from the same limiting solution plus the definition of Δ_P in Eq 63. From Eqs 83 and 84

$$\frac{P_O}{\epsilon_0 b}\left(\frac{\partial \Delta_P}{\partial P}\right)_a = k \ln \psi + 2k(\psi - 1) + \alpha n h_3(n) \left(\frac{P}{P_O}\right)^{n-1} \quad (85)$$

To ensure continuity at P_O, this same expression is used for $P \geq P_O$. Values of h_1 and h_3 for the power-law solution are listed in Table 1. These values are converted from Table 1 of Ref *14* using $h_1 = (a/w)g_1$ and

$$h_3 = (a/w)g_3/(1 - a/w) \text{ for } a/w = 3/4$$

Equation 73 can be expressed in nondimensional form for T, involving only the foregoing quantities and the nondimensional combined compliance

$$\bar{C} = EC = E(C_e + C_M) \quad (86)$$

Curves of T as a function of $EJ/(\sigma_0^2 b)$ are shown in Figs. 9 and 10. For the deeply cracked specimen

$$EC_e = L/W + k \ln (W/b) \quad (87)$$

so the value $\bar{C} = 10$ in Fig. 9 can be regarded as being fairly representative of a test specimen with typical dimensions in a rigid test machine. In contrast to the bend specimen of Fig. 5 in the same range of $EJ/(\sigma_0^2 b)$, a decrease in strain hardening increases T, that is, decreases stability. In both cases the effect of strain hardening is quite significant. Only for the bend specimen does T decrease at sufficiently large increasing J; this is most evident from the formula for the perfectly plastic case, Eq 42. The effect of increasing the combined compliance $\bar{C}$ is seen in Fig. 10 for $n = 5$. Here the trends are very similar to those for the bend specimen.

Discussion

Two open questions are the maximum allowable amount of crack growth and the minimum admissible value of the nondimensional parameter ω to ensure J-controlled growth to a reasonable approximation. For a fully yielded specimen with ligament b, the most relevant material-based estimate of ω just following initiation is Eq 56, that is

$$\omega = \frac{b}{J_{Ic}}\frac{dJ}{da} = \left(\frac{\sigma_0^2 b}{EJ_{Ic}}\right) T_{mat}$$

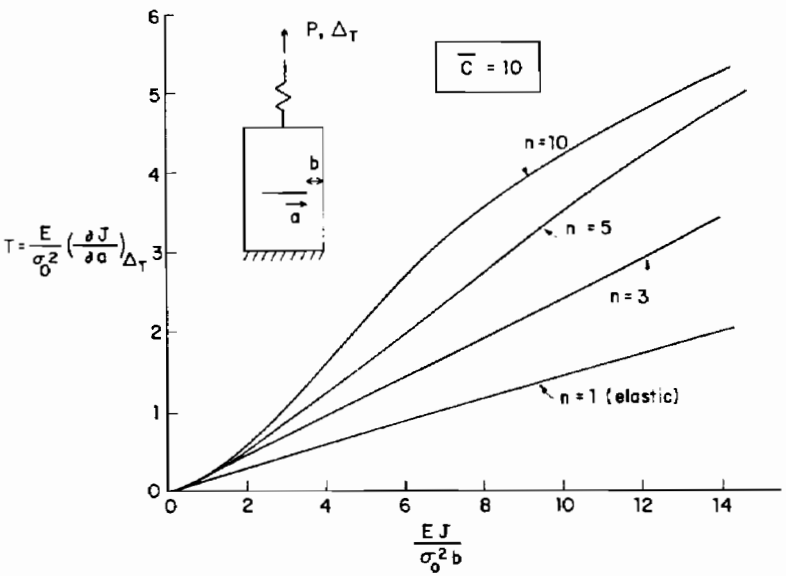

FIG. 9—*Curves of* T *as a function of* EJ/(σ_0^2b) *for various levels of strain hardening index* n *for a deeply center-cracked plane-stress tension specimen. Nondimensional combined compliance is* $\bar{C}$ = *10, corresponding to a typically dimensioned specimen in a rigid test machine (see text).*

The range of this parameter for the steels listed by Paris et al ([*1*] Appendix II) is roughly $0.1 < \omega < 100$ with most entries satisfying $\omega > 10$. Thus it does seem likely that there will be an important class of metals whose properties are such that a limited amount of growth can be analyzed, both for equilibrium and stability, using the deformation theory J. However, Landes and Begley ([*16*] and private communications) have noted that the J-integral resistance curves for compact or bend specimens have a different slope, dJ_{mat}/da, than those for center-cracked specimens. On the other hand, their curves were plotted with J-values which were uncorrected for effects of crack length changes, such as is illustrated by the second term in Eq 31. Moreover, in their tests ω was not evaluated and their ligaments sizes, b, did not quite meet the other requirements, as illustrated by Eq 12. In addition, they report unsymmetrical crack extension for the two crack tips in their center-crack specimens. Nevertheless, this perplexing point cannot be dismissed; thus further exploration is warranted until a reasonable explanation is found.

It should be most interesting to compare results from deformation theory calculations and flow theory calculations for precisely the same prescribed growth conditions. In this way it should be possible to learn more about the

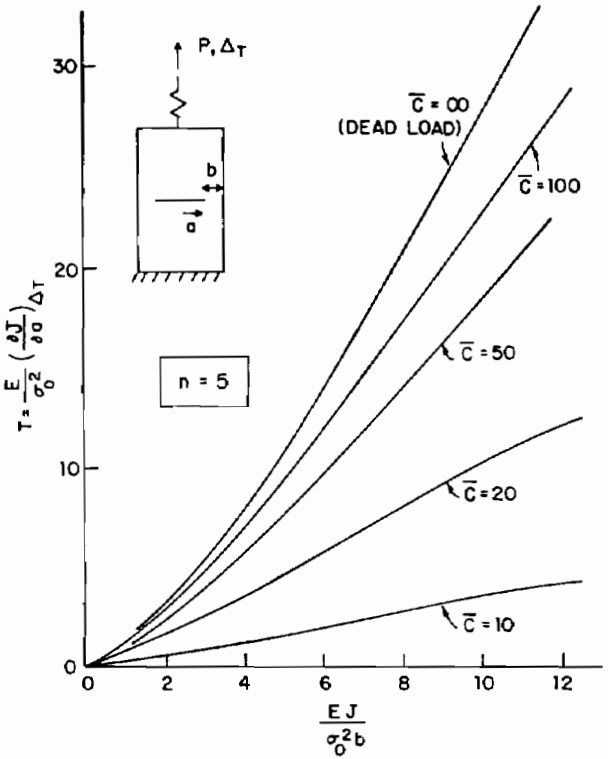

FIG. 10—*Influence of combined compliance on T for deeply center-cracked plane-stress tension specimen for strain-hardening index* n = 5.

influence of strain hardening and configuration on the minimum permissible value of ω. It is worth bearing in mind that the simplest flow theories of plasticity, based on a smooth yield surface, have limitations which may also be important in the analysis of crack growth. In particular, certain of the incremental moduli tend to be overestimated by the simplest flow theories, leading in some problems to unrealistically high resistance to plastic deformation. In this connection, we also note that our argument requiring $\omega \gg 1$ may be relaxed somewhat by appealing to the total loading concept for justifying deformation theory as discussed by Budiansky [*6*].

In this paper we have emphasized the analysis of deeply cracked configuration because relatively simple formulas for T can be obtained which, in some instances, are directly applicable to test specimens. Work is underway [*17*] using estimation procedures based on the power-law solutions to predict T for arbitrary crack lengths. At the moment, however, power-law solutions are available only for a very few configurations and, in plane strain, only for the center-cracked strip [*18*].

Finally, within this work, suggestions have been made for methods of analysis of load-displacement records which permit establishing a material's J-integral R-curve without direct measurements of crack length changes. Though a special case of this approach was used with success in earlier tests [*1*], the method is unexplored, but holds great promise for simplifying testing. Indeed, those methods can be extended to eliminate the requirement for deeply cracked specimens, but that will be a topic for subsequent discussions. Furthermore, since those methods determine dJ_{mat}/da from load-displacement relations as influenced by crack growth, they are a most natural way to assess material parameters affecting stability. That is true because stability itself depends directly on the influence of crack growth on load-displacement behavior, as is observed throughout the analysis herein.

Acknowledgments

The first author (J. W. H.) acknowledges support of this work by the National Science Foundation, Grant No. ENG76-04019, and in part by the Division of Applied Sciences of Harvard University. The second author (P. C. P.) acknowledges the support of this work by the United States Nuclear Regulatory Commission, Contract No. NRC-03-77-029 with Washington University. The work was also significantly assisted by many stimulating discussions with several co-workers, including J. R. Rice, H. Tada, A. Zahoor, H. Ernst, C. F. Shih, and R. Gamble.

References

[*1*] Paris, P., Tada, H., Zahoor, A., and Ernst, H., "A Treatment of the Subject of Tearing Instability," U. S. Nuclear Regulatory Commission Report NUREG-0311, Aug. 1977. (See also papers in this publication by these authors.)

[*2*] *Fracture Toughness Evaluation by R-Curve Methods, ASTM STP 527,* American Society for Testing and Materials, 1974.

[*3*] McClintock, F. and Irwin, G. R. in *Fracture Toughness Testing and Its Applications, ASTM STP 381,* American Society for Testing and Materials, 1965, pp. 84–113.

[*4*] Rice, J. R. in *Mechanics and Mechanisms of Crack Growth*, British Steel Corp., 1973.

[*5*] Rice, J. R. in *Fracture,* Vol. 2, Academic Press, New York, 1968.

[*6*] Budiansky, B., *Journal of Applied Mechanics,* Vol. 26, 1959, pp. 259–264.

[*7*] Begley, J. A. and Landes, J. D. in *Fracture Analysis, ASTM STP 560,* American Society for Testing and Materials, 1974, pp. 170–186.

[*8*] Hutchinson, J. W., *Journal of the Mechanics and Physics of Solids,* Vol. 16, 1968, pp. 13–31.

[*9*] Rice, J. R. and Rosengren, G. F., *Journal of the Mechanics and Physics of Solids*, Vol. 16, 1968, pp. 1–12.

[*10*] McClintock, F. A. in *Fracture,* Vol. 3, Academic Press, New York, 1971.

[*11*] Landes, J. D. and Begley, J. A. in *Fracture Toughness, ASTM STP 514,* American Society for Testing and Materials, 1972, pp. 1–20 and 24–39.

[*12*] Shih, C. F., de Lorenzi, H. G., Andrews, W. R., Van Stone, R. H., and Wilkinson, J. P. D., "Methodology for Plastic Fracture," Fourth Quarterly Report by General Electric Co. to Electric Power Research Institute, 6 June 1977.

[*13*] Rice, J., Paris, P., and Merkle, J. in *Progress in Flaw Growth and Fracture Toughness Testing, ASTM STP 536,* American Society for Testing and Materials, 1973, pp. 231–245.

4] Shih, C. F. and Hutchinson, J. W., *Journal of Engineering Materials and Technology*, Vol. 98, 1976, pp. 289-295.
5] Tada, H., Paris, P. C., and Irwin, G. R., *The Stress Analysis of Cracks Handbook*, Del Research Corp., 226 Woodbourne Drive, St. Louis, Mo., 1973.
6] Begley, J. A. and Landes, J. D., *International Journal of Fracture Mechanics*, Vol. 12, No. 5, Oct. 1976.
7] Zahoor, A., work in progress.
8] Goldman, N. L. and Hutchinson, J. W., *International Journal of Solids and Structures*, Vol. 2, 1975.